J Mol Model (2013) 19:397–406
DOI 10.1007/s00894-012-1567-0

ORIGINAL PAPER

Quantum chemical investigation of the intra- and intermolecular proton transfer reactions and hydrogen bonding interactions in 4-amino-5-(2-hydroxyphenyl)-2*H*-1,2,4-triazole-3(4*H*)-thione

Namık Özdemir

Received: 21 February 2012 / Accepted: 9 August 2012 / Published online: 1 September 2012

Abstract The intramolecular thione-thiol tautomerism and intermolecular double proton transfer reaction of the hydrogen-bonded thione and thiol dimers in the title triazole compound were studied at the B3LYP level of theory using 6−311++G(d,p) basis function. The influence of the solvent on the single and double proton transfer reactions was examined in three solvents (chloroform, methanol and water) using the polarizable continuum model (PCM) approximation. The computational results show that the thione tautomer is the most stable isomer with a very high tautomeric energy barrier both in the gas phase and in solution phase, indicating a quite disfavored process. The solvent effect is found to be sizable with increasing polarity. In the double proton transfer reaction, the thione dimer is found to be more stable than thiol dimer both in the gas phase and in solution phase. The energetic and thermodynamic parameters of the double proton transfer process show that the double proton exchange from thione dimer to thiol dimer is thermodynamically unfavored. However, the exchange from thiol dimer to thione dimer for the gas phase and water phase seems to be feasible with a low barrier height and with a negative value in enthalpy and free energy changes. In addition, the hydrogen bonding interactions were analyzed in the gas phase regarding their geometries and energies. It is found that all complex formations are enthalpically favored, and the stability of the H-bonds comes in the order of S1—H2···N2 > N2—H2···S1 > N3—H3B···O1. Finally, non-linear optical properties were carried out at the same calculation level in the gas phase.

Keywords Density functional calculations · Double proton transfer reaction · Hydrogen bonding · Solvent effect · Thione-thiol tautomerism · 1,2,4-triazole

Introduction

1,2,4-triazole rings are typically planar 6π-electron aromatic systems, featuring an extensive chemistry [1, 2]. 1,2,4-triazole and its derivatives represent one of the most biologically active classes of compounds, possessing a wide spectrum of activities, including anti-inflammatory [3, 4], antiviral [5], analgesic [6], antimicrobial [7], anticonvulsant [8], anticancer [9], antioxidant [10], antitumorial [11] and antidepressant activity [12], the last usually being explored by the forced-swim test [13, 14]. Furthermore, some of the complexes containing 1,2,4-triazole ligands have rather peculiar structures and specific magnetic properties [15–18].

Studies of noncovalently bonded molecular clusters are of great interest for contemporary chemical science from both fundamental and practical perspectives. Among the various types of intermolecular interactions, the hydrogen bond is arguably the most important, due to its widespread occurrence and strength [19–21]. The study of relatively simple organic molecules is a vital source of information regarding the underlying physical forces that hold these molecules together. In particular, in the solid state, the study of crystal structures yields information on the intermolecular forces. The intermolecular hydrogen bonding which is so often present in such systems plays an important role in forming anisotropic interactions, and, for example, the hydrogen transfer through hydrogen bonds between molecules enables charge and energy transfer in solid chemical and

Electronic supplementary material The online version of this article (doi:10.1007/s00894-012-1567-0) contains supplementary material, which is available to authorized users.

N. Özdemir (✉)
Department of Physics, Faculty of Arts and Sciences,
Ondokuz Mayıs University,
55139, Kurupelit,
Samsun, Turkey
e-mail: namiko@omu.edu.tr

biological systems and has widespread implications for issues as diverse as ferroelectrics, electrochemical processes and enzyme action [22].

In recent years, intra- or intermolecular proton transfer has been a topic of much interest because of its importance in many chemical and biological processes [23–27]. A large number of theoretical and experimental investigations have been carried out to enrich the information regarding the possible mechanisms of proton transfer, and tautomeric equilibria, and relevant properties associated with proton transfer [23–33]. In particular, the role played by the solvent in intra- or intermolecular proton transfer reactions is known to be crucial [34].

Because of conclusive evidence on significant biological activities of 1,2,4-triazole-3-thiones, synthesis of the substituted derivatives of 1,2,4-triazole-3-thione have been of interest [35]. A common question has dealt extensively with intramolecular tautomerization encountered in such structures [36–38]. These compounds can exist in two major tautomeric forms that exhibit different reactivities [12, 39–41]. The thione-thiol tautomerism of these compounds remains as a matter of controversy, because it is not straightforward to determine which of the two forms is present. The prototropic tautomerism of 1,2,4-triazole-3-thione parent and its disubstituted derivatives containing benzyl and pyridyl groups is of great importance in many areas of chemistry and biochemistry [12, 35–41]. The knowledge of the relative stabilities of tautomeric forms as well as of the conversion from one tautomeric form to another is also important from the point of view of structural chemistry. In addition, knowing how the tautomerization energies change in various solvents gives an insight into the influence of solvents on molecular stability and reactivity. So, it is worth studying the possibility of tautomerization in the parent molecule of 1,2,4-triazole-3-thione and its disubstituted derivatives using high accuracy methods [42].

The present study focuses on a detailed theoretical study of the intramolecular single proton transfer (thione-thiol tautomerism) and intermolecular double proton transfer reactions (between hydrogen-bonded thione and thiol dimers), and hydrogen bonding interactions in the title compound. The calculations were performed at the DFT/B3LYP level of theory using the 6−311++G(d,p) basis function. Furthermore, solvent effects are estimated through the use of a polarized continuum model (PCM) at the same calculation level.

Computational details

All geometries were fully optimized in the ground state using the Berny algorithm [43] and default convergence criteria. The stationary structures and transition state were confirmed by establishing that the matrixes of the energy second derivatives (Hessians) have zero and one negative eigenvalue, respectively. The cartesian coordinates of the X-ray structure were used as the starting geometry for the theoretical calculations. All calculations were performed by means of the Gauss View molecular visualization program [44] and GAUSSIAN 03 program package [45] using the spin-restricted hybrid density functional theory (B3LYP) [46, 47] method with the 6−311++G(d,p) [48, 49] basis set. This method has been demonstrated to be able to predict reliable geometries and vibrational frequencies for hydrogen-bonded systems [50–53]. The binding energies were calculated using the supermolecule approach [54, 55], and corrected for basis set superposition error (BSSE) via the standard counterpoise method [56]. In order to investigate the solvent effects, I have also carried out calculations in three kinds of solvents [ε=4.90, chloroform ($CHCl_3$); ε=32.63, methanol (CH_4O); ε=78.39, water (H_2O)] at the same level using polarizable continuum model (PCM) [57–60] method. Although the use of doubly diffuse functions in the basis set in conjunction with a continuum model of solvent might lead to some over-polarization, the obtained results (see below) show consistent trends ranging from gas phase to highly polar medium indicating no over-polarization issues [61, 62]. The thermodynamic parameters were obtained from the frequency analyses of the optimized structures, and were calculated using the thermodynamic equations and $\Delta G = \Delta H - T\Delta S$ [63, 64].

Results and discussion

Theoretical structures

The molecular structure of the title compound [65], which is shown in Fig. 1, was optimized by energy-minimization with the density functional theory (DFT) method with the 6−311++G(d,p) basis set. Some selected geometrical

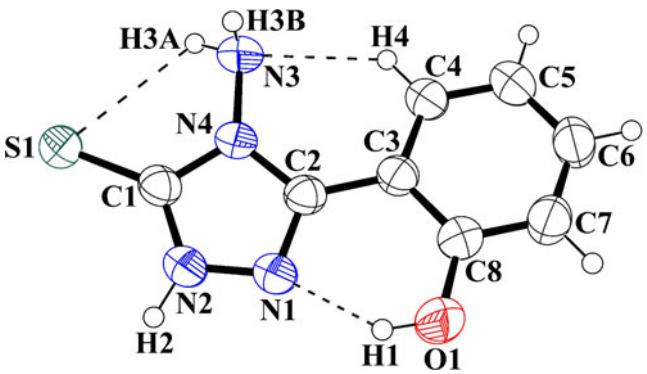

Fig. 1 The solid state structure of the title compound [65]. The dashed lines represent the intramolecular O1—H1···N1, C4—H4···N3 and N3—H3A···S1 hydrogen bonds

parameters experimentally obtained and theoretically calculated both in the gas phase and in solution phase are listed in Table 1 (see the Supplementary data for full table). Although two conformations of the compound can be drawn by a rotation around the C2—C3 bond, only one of these two conformers is studied here, which is the most stable and accords with the X-ray structure.

As can be seen in Table 1, agreement between the calculated structures and the experimentally determined X-ray crystal structure is satisfactory. Bond distances agree within ca 0.13 Å, while the largest deviation of the bond angles appears to be about 3.72°. Interestingly, the biggest difference in bond distances and angles takes place at the N2—H2 unit. When the X-ray structure of the title compound is compared with its optimized counterparts, some conformational discrepancies are observed between them. According to X-ray study, the dihedral angle between the triazole and benzene rings of the title molecule is 10.95(12)°. This angle is calculated at 0.026° for the gas phase, while it is found to be 0.147, 2.969 and 0.059° in going from chloroform to water for solution phase, respectively.

A logical method for globally comparing the structures obtained with the theoretical calculations is by superimposing the molecular skeleton with that obtained from X-ray diffraction, giving RMSE's of 0.108, 0.110, 0.080 and 0.109 Å, respectively, in going from the gas phase to solution phase.

The molecular structure of the title compound contains three intramolecular interactions. The experimental and calculated geometric parameters belonging to these interactions are collected in Table 2. As can be seen from the table, there is good agreement between the experimental and theoretical values, except for N3—H3A···S1 contact. The main reason of the difference in this contact is that the other proton (H3B) on atom N3 participates in an intermolecular hydrogen bonding, and therefore the NH_2 group rotates around the N3—N4 bond in the solid state. It was noted that the experimental results belong to solid phase and theoretical calculations correspond to the isolated molecule in the gas and solution phases. In the solid state, the existence of the crystal field along with the intermolecular interactions has connected the molecules together, which result in the differences of structural parameters between the calculated and experimental values.

The mean linear polarizability (α_{tot}) and first-order hyperpolarizability (β_{tot}) of the two tautomers were calculated at the B3LYP/6−311++G(d,p) level in the gas phase. The calculated values of α_{tot} and β_{tot} are 23.603 $Å^3$ and 4.282×10^{-30} cm^5/esu for the thione tautomer, and 22.849 $Å^3$ and 4.578×10^{-30} cm^5/esu for the thiol tautomer, respectively. Urea is one of the prototypical molecules used in the study of the NLO properties of molecular systems. Therefore it was used frequently as a threshold value for comparative purposes. The values of α_{tot} and β_{tot} of urea are

Table 1 Experimental and optimized structural parameters of the thione-thiol tautomers and transition state of the title compound

Parameters	X-ray	Gas phase			Chloroform (ε=4.90)			Methanol (ε=32.63)			Water (ε=78.39)		
		Thione	TS	Thiol	Thione	TS	Thiol	Thione	TS	Thiol	Thione	TS	Thiol
Bond lengths (Å)													
S1—C1	1.6773(18)	1.664	1.721	1.762	1.679	1.726	1.759	1.685	1.728	1.757	1.687	1.728	1.757
S1—H2	–	–	–	1.348	–	–	1.365	–	–	1.374	–	–	1.376
N1—C2	1.309(2)	1.315	1.321	1.320	1.315	1.322	1.321	1.316	1.323	1.322	1.316	1.323	1.322
N2—C1	1.329(2)	1.352	1.318	1.302	1.345	1.318	1.307	1.343	1.318	1.309	1.342	1.319	1.309
N2—H2	0.90(2)	1.007	–	–	1.021	–	–	1.027	–	–	1.028	–	–
N3—N4	1.399(2)	1.396	1.400	1.398	1.396	1.400	1.398	1.396	1.400	1.398	1.396	1.400	1.398
Bond angles (°)													
S1—C1—N2	130.49(13)	130.38	109.72	127.62	129.55	109.07	127.97	129.26	108.84	128.02	129.20	108.80	128.12
S1—C1—N4	125.91(13)	127.49	141.91	121.33	127.56	142.37	121.26	127.55	142.54	121.33	127.56	142.56	121.23
C1—S1—H2	–	–	–	92.73	–	–	93.66	–	–	93.95	–	–	93.99
N1—N2—C1	112.96(14)	113.71	110.11	106.29	113.31	109.96	106.36	113.13	109.90	106.38	113.10	109.89	106.36
N1—N2—H2	117.0(15)	120.72	–	–	120.53	–	–	120.41	–	–	120.41	–	–
C1—N2—H2	129.1(15)	125.56	–	–	126.16	–	–	126.45	–	–	126.49	–	–
N2—C1—N4	103.55(14)	102.14	108.37	111.05	102.89	108.56	110.77	103.19	108.62	110.66	103.25	108.63	110.65
N2—N1—C2	105.47(14)	106.11	107.03	110.13	106.19	106.84	109.86	106.22	106.75	109.75	106.24	106.75	109.72
N3—N4—C1	123.64(14)	123.14	126.14	126.90	124.28	126.65	127.10	124.66	126.83	127.14	124.68	126.84	127.07
C1—N4—C2	109.14(13)	109.50	105.94	105.11	109.03	105.85	105.38	108.85	105.82	105.50	108.82	105.82	105.53

ε = dielectric constant

Table 2 Experimental and optimized geometries of intramolecular hydrogen bonds in the title compound

Method	ε	D—H (Å)	H···A (Å)	D···A (Å)	D—H···A (°)
		O1—H1···N1			
Experimental		0.86(3)	1.89(3)	2.611(2)	140(2)
B3LYP	1	0.979	1.769	2.622	143.59
PCM	4.90	0.981	1.760	2.615	143.54
	32.63	0.983	1.759	2.613	143.30
	78.39	0.983	1.761	2.614	143.08
		C4—H4···N3			
Experimental		0.97(2)	2.35(2)	3.013(3)	125(2)
B3LYP	1	1.079	2.266	3.037	126.73
PCM	4.90	1.079	2.260	3.029	126.53
	32.63	1.080	2.263	3.029	126.25
	78.39	1.080	2.261	3.029	126.40
		N3—H3A···S1			
Experimental		0.91(3)	2.73(4)	3.1319(18)	108(3)
B3LYP	1	1.019	3.029	3.174	88.71
PCM	4.90	1.023	3.084	3.203	87.32
	32.63	1.025	3.087	3.213	87.66
	78.39	1.025	3.104	3.214	86.79

ε = dielectric constant

5.042 Å^3 and 0.765×10^{-30}cm^5/esu obtained at the same level. Theoretically, the first-order hyperpolarizability of both tautomers is of ca six times the magnitude of urea. According to these results, both tautomers are a good candidate of NLO material.

Intramolecular single proton transfer reaction (thione-thiol tautomerism)

As shown in Fig. 2, two tautomeric forms may exist for the title molecule, the thione (NH) and thiol (SH) forms. The first with a C1 =S1 double bond and latter with the endocyclic double bond C1 = N2. Some selected structural parameters belonging to the thione, thiol and transition state (TS) geometries of the title compound optimized at the B3LYP/6−311++G(d,p) level are listed in Table 1, while the energies of the thione and thiol forms, energy differences and activation energies are given in Table 3. The calculated imaginary vibrational frequency of the transition state is 1656i cm^{-1} for the gas phase, 1722i cm^{-1} for chloroform, 1751i cm^{-1} for methanol and 1756i cm^{-1} for water.

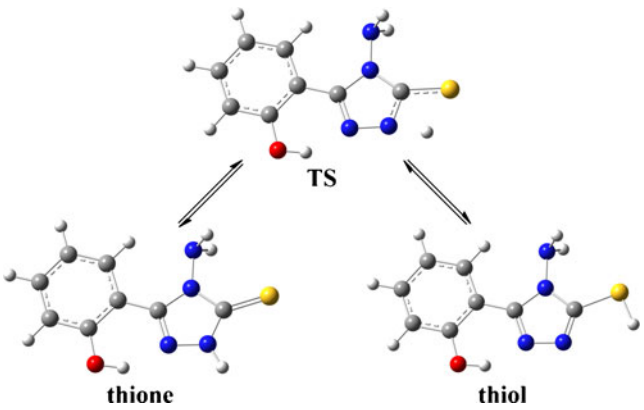

Fig. 2 The mechanism for tautomerization of 1,2,4-triazole-3-thione to 1,2,4-triazole-3-thiol and corresponding transition structure (TS)

Due to the migration of a hydrogen atom from atom N2 to atom S1, some changes are observed in the structure. The distance between atoms S1 and H2 decreases upon the proton transfer thione → TS → thiol. It can be concluded that the N2—H2 bond is broken, and an S1—H2 bond (1.348 Å in the gas phase, and 1.365, 1.374 and 1.376 Å in going from chloroform to water, respectively) is formed during the intramolecular proton transfer process in the compound. As can be seen from Table 1, the S1—C1 and N1—C2 distances increase, while the N2—C1 distance decreases in the proton transfer thione → TS → thiol. Besides, the S1—C1—N2, S1—C1—N4, N1—N2—C1 and C1—N4—C2 angles contract as the N2—C1—N4, N2—N1—C2 and N3—N4—C1 angles expand.

The N2···H2 and S1···H2 distances for TS structure are found to be 1.367 and 1.744 Å in the gas phase, 1.365 and 1.740 Å in chloroform, 1.364 and 1.739 Å in methanol, and 1.363 and 1.739 Å in water, respectively. When the transition structure is globally compared with both the thione and thiol tautomers, the obtained RMSE's are 0.124, 0.122, 0.122 and 0.122 Å for thione tautomer, 0.125, 0.132, 0.141 and 0.137 Å for thiol tautomer in going from the gas phase to water phase, respectively. From a structural point of view, all results indicate that the transition state resembles more the thione than the thiol tautomer, with the transferred proton closer to that observed for the thione than for the thiol form. The parameters given in Table 1 also show that both tautomers and the transition state connecting them are completely planar. This fact could be evidenced by referring to Table 1 where the selected torsion angles are approximately 0 or 180° which show completely planar geometries. By taking a closer look at the structures and imaginary frequency of transition state, it reveals that even during the tautomerization process, the proton (H2) has been transferred from N2 to S1 in the molecular plane.

The energy profile of the single proton transfer process (thione-thiol tautomerism) is shown in Fig. 3. The tautomerization energy, as shown in Fig. 3, was calculated as the energy differences between the tautomers and the transition state. The energy differences between the two tautomers were calculated to be −61.53, −60.04, −59.27 and −59.12 kJmol^{-1} in going from the gas phase to water phase, respectively. Considering the ground state energy of the thione and thiol tautomers as well as the tautomerization energies in Table 3 show that the thione form is more stable

Table 3 Energies of the title 1,2,4-triazol-3-thione compound and its thiol form in hartree, and energy differences, activation energies and thermodynamic parameters in kJmol^{-1}

Method	ε	Thione	Thiol	ΔE	E_a(f)	E_a(r)	ΔH_{298}(f)	ΔG_{298}(f)	$T\Delta S_{298}$(f)	ΔH_{298}(r)	ΔG_{298}(r)	$T\Delta S_{298}$(r)
B3LYP	1	−1002.25703058	−1002.23359560	−61.53	197.04	135.51	178.72	179.60	−0.88	127.40	127.91	−0.51
PCM	4.90	−1002.27601453	−1002.25314579	−60.04	219.18	159.14	204.35	205.06	−0.71	154.28	154.37	−0.09
	32.63	−1002.28385470	−1002.26127842	−59.27	229.15	169.88	216.31	217.69	−1.37	167.06	168.20	−1.14
	78.39	−1002.28497799	−1002.26246215	−59.12	230.49	171.37	215.50	225.35	−9.86	166.39	175.62	−9.24

ε = dielectric constant, $\Delta E = E_{thione} - E_{thiol}$, E_a(f) = forward activation energy, E_a(r) = reverse activation energy

than the thiol case in both the gas phase and in solution phase.

The relative energies of the TS with respect to the thione tautomer were obtained as 197.04, 219.18, 229.15 and 230.49 kJmol^{-1}, while the reverse reaction barriers were calculated as 135.51, 159.14, 169.88 and 171.37 kJmol^{-1} in the gas phase, in chloroform, in methanol, and in water, respectively. These values show that considerable high energy is necessary for both the forward and the reverse proton transfer to occur. In both cases, the barrier height increases in going from the gas phase to water phase. High barrier energies in Table 3 suggest an unfavorable tautomerism both in the gas phase and in solution phase. It can be easily said that the stronger the dipole moment of the solvent, the higher the barrier to the proton transfer process.

The standard enthalpy and free energy changes for the single proton transfer are also listed in Table 3. As can be seen from the table, the large positive standard enthalpy and free energy changes for both the forward and the reverse proton transfer demonstrate that the thione → thiol and thiol → thione processes are highly endothermic reactions both in the gas phase and in solution phase. In conclusion, the single transfer is a quite disfavored process or not a spontaneous process.

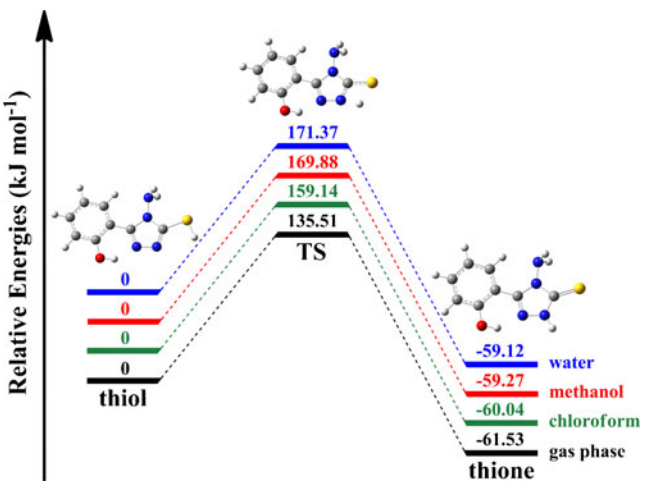

Fig. 3 Relative energy profile of the single proton transfer process (thione-thiol tautomerism) in the gas phase and various solvents

Intermolecular double proton transfer reaction

In the crystal structure of the title compound [65], centrosymmetric dimers (thione dimer) are formed via N—H···S hydrogen bonds generating an $R_2^2(8)$ ring [66], that can affect the tautomeric equilibrium [67]. Here, the intermolecular double proton transfer between the thione and thiol dimers has been investigated both in the gas phase and in solution phase at the same level of theory. Optimizations of the dimers were performed without symmetry constraints.

Some selected structural parameters belonging to the thione and thiol dimers, and transition state (TS) geometries optimized at the B3LYP/6−311++G(d,p) level are listed in Table 4 (see the Supplementary data for full table), while the energies of the thione and thiol dimers, energy differences and activation energies are given in Table 5. The calculated imaginary vibrational frequency of the transition state is 183i cm^{-1} for the gas phase, 291i cm^{-1} for chloroform, 530i cm^{-1} for methanol and 546i cm^{-1} for water.

The most remarkable changes in bond lengths and bond angles in going from the monomer structures to the cyclic dimeric structures can be summarized as follows. In the thione dimer, the S1—C1 and N2—H2 bond lengths increase as a result of the N—H···S interactions, while the N2—C1 and N4—C1 distances decrease. In addition, the S1—C1—N2, C1—N2—H2 and N2—C1—N4 angles become larger, while the S1—C1—N4, N1—N2—C1 and C1—N4—C2 angles become smaller. In the thiol dimer, the S1—H2 and N2—C1 bond lengths increase as a result of the S—H···N interactions, while the S1—C1 distance decreases. Also, the S1—C1—N2, C1—S1—H2, N1—N2—C1 and C1—N4—C2 angles expand as the N2—C1—N4, N2—N1—C2 and N3—N4—C1 angles contract. The average N2···H2 and S1···H2 distances for TS structure are found to be 1.576 and 1.465 Å in the gas phase, 1.545 and 1.479 Å in chloroform, 1.581 and 1.472 Å in methanol, and 1.586 and 1.471 Å in water, respectively.

The mechanism of the double proton transfer process between the thione and thiol dimers is given in Fig. 4, while the energy profile is shown in Fig. 5. The energy differences between the two dimers were calculated to be −115.42, −102.42, −111.37 and −127.61 kJmol^{-1} in going from gas

Table 4 Optimized structural parameters of the thione and thiol dimers, and transition state of the title compound

Parameters	Gas phase			Chloroform (ε=4.90)			Methanol (ε=32.63)			Water (ε=78.39)		
	Thione dimer	TS	Thiol dimer	Thione dimer	TS	Thiol dimer	Thione dimer	TS	Thiol dimer	Thione dimer	TS	Thiol dimer
Bond lengths (Å)												
S1—C1	1.683	1.739	1.747	1.687	1.739	1.750	1.692	1.741	1.751	1.692	1.742	1.751
S1—H2	–	–	1.403	–	–	1.390	–	–	1.385	–	–	1.387
N1—C2	1.315	1.318	1.319	1.315	1.319	1.320	1.315	1.319	1.321	1.315	1.319	1.320
N2—C1	1.342	1.314	1.310	1.341	1.316	1.311	1.339	1.316	1.312	1.339	1.316	1.312
N2—H2	1.030	–	–	1.028	–	–	1.028	–	–	1.028	–	–
N4—C1	1.389	1.380	1.380	1.386	1.378	1.377	1.383	1.376	1.376	1.383	1.375	1.377
Bond angles (°)												
S1—C1—N2	131.10	129.47	129.17	130.28	128.93	128.57	129.73	128.89	128.33	129.67	128.86	128.25
S1—C1—N4	125.66	122.16	121.57	126.30	122.75	121.78	126.64	122.78	121.83	126.68	122.80	122.05
C1—S1—H2	–	–	94.30	–	–	94.28	–	–	94.23	–	–	94.15
N1—N2—C1	112.95	108.46	107.67	112.89	108.50	107.31	112.82	108.63	107.11	112.79	108.63	107.25
N1—N2—H2	120.40	–	–	120.42	–	–	120.45	–	–	120.44	–	–
C1—N2—H2	126.65	–	–	126.69	–	–	126.73	–	–	126.76	–	–
N2—C1—N4	103.24	108.38	109.27	103.42	108.32	109.65	103.63	108.33	109.83	103.65	108.34	109.70
N2—N1—C2	106.60	109.10	109.49	106.50	108.90	109.43	106.36	108.72	109.41	106.41	108.71	109.42
N3—N4—C1	123.73	125.84	126.17	124.37	126.28	126.65	124.72	126.49	126.83	124.70	126.52	126.94
C1—N4—C2	108.94	106.56	106.13	108.79	106.55	105.96	108.66	106.51	105.89	108.65	106.50	105.91

ε = dielectric constant

phase to water phase, respectively. The ground state energy of the thione and thiol dimers as well as the energy differences between the two dimers and the transition state in Table 5 show that the thione dimer is more stable than thiol dimer both in the gas phase and in solution phase.

The relative energies of the TS with respect to the thione dimer were obtained as 116.47, 120.31, 130.40 and 131.76 kJ mol^{-1} in the gas phase, in chloroform, in methanol, and in water, respectively. Similar to that of thione-thiol tautomerism, the barrier height increases on going from the gas phase to water phase. It is seen that the stronger the dipole moment of the solvent, the higher the barrier to the proton transfer process. However, there is a discrepancy in the reverse reaction. The reverse reaction has a very low energy barrier with values of 1.05, 17.89, 19.03 and 4.15 kJ mol^{-1} in going from the gas phase to water phase, respectively. As a result, this reaction is much easier than the forward proton transfer, especially in the gas phase and in water.

In the PCM method, the reaction potential includes only electrostatic solute-solvent interactions. However, important effects associated with specific solute-solvent interactions are neglected by the continuum approximation, especially in the description of the proton transfer mechanism in hydrogen-bonded systems. The solvent can control the dynamics of a proton transfer reaction via two distinct types of solute-solvent interactions. The first is long-range solvent polarization interactions and the second is specific short-range hydrogen bonding interactions. In the second case, protic solvents, like water, can accept a proton from the

Table 5 Energies of the thione and thiol dimers of the title 1,2,4-triazol-3-thione compound in hartree, and energy differences, activation energies and thermodynamic parameters in kJ mol^{-1}

Method	ε	Thione dimer	Thiol dimer	ΔE	E_a(f)	E_a(r)	ΔH_{298}(f)	ΔG_{298}(f)	$T\Delta S_{298}$(f)	ΔH_{298}(r)	ΔG_{298}(r)	$T\Delta S_{298}$(r)
B3LYP	1	−2004.53333478	−2004.48937408	−115.42	116.47	1.05	87.72	96.12	−8.40	−6.66	−0.83	−5.83
PCM	4.90	−2004.54668912	−2004.50767866	−102.42	120.31	17.89	84.49	87.04	−2.55	3.35	2.90	0.44
	32.63	−2004.55781754	−2004.51539920	−111.37	130.40	19.03	101.67	105.97	−4.30	10.16	5.78	4.37
	78.39	−2004.55895976	−2004.51035674	−127.61	131.76	4.15	103.31	110.92	−7.61	−5.35	−1.09	−4.26

ε = dielectric constant, $\Delta E = E_{\text{thione dimer}} - E_{\text{thiol dimer}}$, E_a(f) = forward activation energy, E_a(r) = reverse activation energy

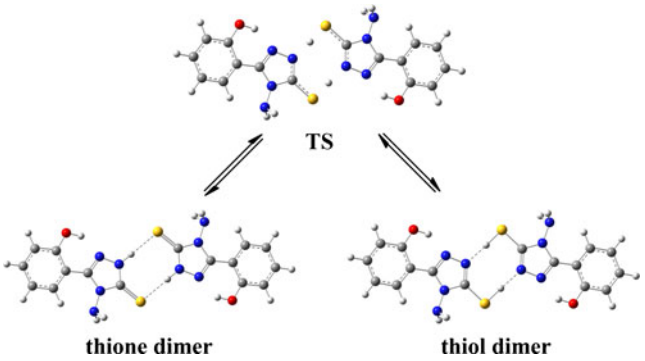

Fig. 4 The mechanism for the double proton transfer process between the thione and thiol dimers and corresponding transition structure (TS)

donor site of the solute molecule and transfer a different proton to the acceptor site on the solute. In this way, the solvent influences the whole reaction path by lowering the energy barrier due to the direct participation of solvent molecule(s) in the proton transfer [68].

The standard enthalpy and free energy changes for the double proton transfer are also listed in Table 5. Similar to those observed in thione-thiol tautomerism, the forward double proton transfer (from thione dimer to thiol dimer) is found to be endothermic with large positive standard enthalpy and free energy changes both in the gas phase and in solution phase. The reverse reaction (from thiol dimer to thione dimer) has a negative value in enthalpy and free energy changes for both the gas phase and water phase, so indicating an exothermic process (a favored process or a spontaneous process). However, a positive change found for chloroform and methanol solvents in the reverse reaction demonstrates an endothermic process, although their barrier heights are relatively low.

When the intramolecular and intermolecular proton transfer reactions are compared, it is easily seen that the

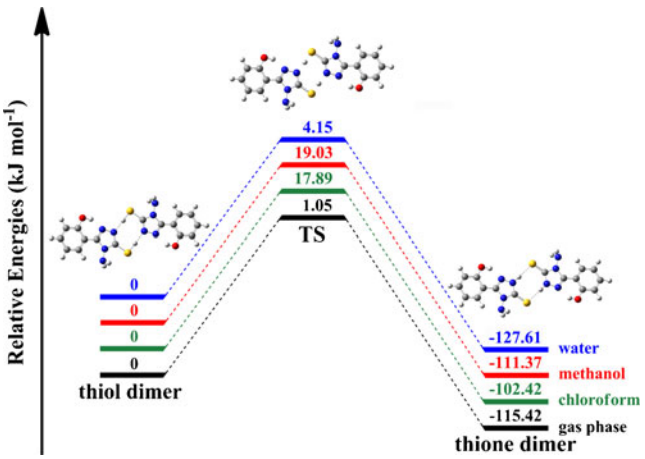

Fig. 5 Relative energy profile of the double proton transfer process between the thione and thiol dimers in the gas phase and various solvents

activation energies for the forward intermolecular proton transfer reaction are almost reduced by a half although the transferred proton number is increased two times. The same trend is also observed in enthalpy and free energy changes.

Intermolecular hydrogen bonding interactions

The geometrical and energetic features of the intermolecular hydrogen bonding interactions observed in the solid state structure of the title compound were investigated at the same level in the gas phase, and the results are tabulated in Table 6 together with its experimental values.

It can be observed from the table that the calculated hydrogen bond lengths are 2.325 and 2.200 Å for N2—H2···S1 and N3—H3B···O1 interactions, respectively, which are shorter than those of X-ray values. Due to the hydrogen bonding, the bond lengths N2—H2 and N3—H3B are found to be slightly increased by 0.022 and 0.003 Å, respectively, as compared to those in free thione tautomer (N3—H3B = 1.019 Å) in the gas phase. The N2—H2···S1 angle is found to be almost linear at 179.33° being characteristic of a strong hydrogen bond, while the N3—H3B···O1 angle is less linear at 166.33° being indicative of a weaker hydrogen bond. These are consistent with the computed BSSE corrected binding energies.

The S atom has been known to act as proton acceptor in H-bonds, but there is even less information about S as a proton donor. Desiraju and Steiner [21] point out that S—H···N H-bonds occur in crystals only very rarely. So, investigation of the intermolecular S—H···N H-bonds in the thiol dimer may be useful since very limited experimental [69] or theoretical [70–74] information about S as a proton donor is available in the literature. Table 6 includes the values of the geometric and energetic parameters for intermolecular S1—H2···N2 H-bond. The S1—H2···N2 interaction leads to an increase in the S—H bond length by 0.05 Å, as compared to that in free thiol tautomer. The calculated hydrogen bond length is 1.814 Å, and the collinear bond angle is very close to being linear at 178.24°.

The computational results show that the cyclic dimer formed by paired N2—H2···S1 interactions is found to be the thermodynamically most stable as compared to the other dimer (NHO) formed by one N3—H3B···O1 interaction, the difference between their total energies being −25.22 kJ mol^{-1}. According to the total energies, the relative order of stability between the three dimers is thione dimer > NHO > thiol dimer. As can be seen from Table 6, the BSSE corrected binding energies are calculated to be −26.478 and −24.166 kJmol^{-1} for the N2—H2···S1 and N3—H3B···O1 interactions, respectively. Hence, the N2—H2···S1 hydrogen bond is stronger than the N3—H3B···O1 bond. Additionally one can observe that S1—H2···N2 H-bonds in thiol

Table 6 Intermolecular H-bond geometries, interaction energies and thermodynamic parameters ($kJmol^{-1}$) in the gas phase

Parameters	N2—H2···S1		N3—H3B···O1		S1—H2···N2
	Experimental	Theoretical	Experimental	Theoretical	Theoretical
D—H (Å)	0.90(2)	1.029	0.88(4)	1.022	1.398
H···A (Å)	2.34(2)	2.325	2.37(4)	2.200	1.814
D···A (Å)	3.2400(16)	3.353	3.083(2)	3.203	3.212
D—H···A (°)	174(2)	179.33	138(3)	166.33	178.24
E	–	−27.557	–	−27.014	−33.553
E_{CP}	–	−26.478	–	−24.166	−31.603
E^{def}	–	2.326	–	4.904	4.492
E^{opt}	–	−24.152	–	−19.262	−27.111
ΔH_{298}	–	−43.58	–	−19.64	−52.24
ΔG_{298}	–	−1.32	–	−0.65	−1.94
$T\Delta S_{298}$	–	−42.26	–	−18.99	−50.30

E = uncorrected binding energy, E_{CP} = BSSE corrected binding energy, E^{def} = deformation energy, E^{opt} = BSSE corrected total interaction energy

dimer are stronger than the corresponding N2—H2···S1 bonds in thione dimer; this is not surprising and in line with the Leffler-Hammond postulate [75, 76], since the corresponding hydrogen bonds are stronger for systems closer to the transition state.

The standard enthalpy and free energy changes for the three complex formations are also listed in Table 6. The values of the standard enthalpies show that all complex formations are enthalpically favored (exothermic). The values of $T\Delta S_{298}$ imply large entropy changes during the complex formations. Using the ΔG_{298} values, the complexes follow the next stability pattern:

$$\text{S1—H2}\cdots\text{N2} > \text{N2—H2}\cdots\text{S1} > \text{N3—H3B}\cdots\text{O1}.$$

This pattern shows that the supersystem formed by the S1—H2···N2 interaction is the most stable one, which is in an agreement with the H-bond lengths and strengths discussed above. If one takes into account the deformation energy due to the process of complexation, it is seen that the binding energies become weaker.

Conclusions

In this paper, I have reported the results of theoretical investigations of the structural parameters, intramolecular single proton transfer reaction (thione-thiol tautomerism), intermolecular double proton transfer reaction (between hydrogen-bonded thione and thiol dimers), and hydrogen bonding interactions in thione and thiol tautomers of the title 1,2,4-triazole compound using the B3LYP/6−311++G (d,p) method. The solvent effect on the structures and single and double proton transfer reactions was also studied in three kinds of solvents (chloroform, methanol and water). The major conclusions to be gleaned from this work are the following:

1. The structural parameters of the title molecule calculated in the gas phase and in solvents are in very good correspondence with X-ray experimental data. The best geometrical parameters are obtained for methanol solvate in solution phase with an RMS overlay error of 0.080 Å. The predicted NLO properties of the two tautomers are greater than the ones of urea. So, both tautomers are a good candidate as second-order NLO material.
2. It is determined that the thione form is the predominant tautomer both in the gas phase and in solution phase. The predicted energy difference between thione and thiol tautomers is within the range ca 59–62 $kJmol^{-1}$, while the activation energy of thione-thiol tautomerization process is within the range ca 197–231 $kJmol^{-1}$ for thione → thiol reaction, and within the range ca 136–171 $kJmol^{-1}$ for thiol → thione reaction. The barrier height for both the forward and reverse single proton transfer reaction increases upon shifting from the gas phase to water phase. Thus, the tautomerization does not occur from the thermodynamic and kinetic points of view both in the gas phase and in solution phase. These findings are also confirmed by large positive standard enthalpy and free energy changes.
3. When the dimerization of the two tautomers is investigated, the thione dimer is found to be more stable than thiol dimer both in the gas phase and in solution phase, the energy differences being within the range ca 102–128 $kJmol^{-1}$. For the double proton transfer process from the thione dimer to thiol dimer, the barrier height is within the range ca 116–132 $kJmol^{-1}$ indicating an unfavored process with large positive standard enthalpy

and free energy changes. However, very low energy barrier is found for the double proton transfer process from the thiol dimer to thione dimer, within the range ca 1–19 kJmol^{-1}. However, only the transfer process in the gas phase and in water phase is allowed by a negative value in enthalpy and free energy changes indicating an exothermic process.

4. All complexations formed by intermolecular N2—H2···S1, N3—H3B···O1 and S1—H2···N2 H-bonds are enthalpically favored. Comparing the values of uncorrected binding energies (E), BSSE corrected binding energies (E_{CP}) and BSSE corrected total interaction energies (E^{opt}), the stability of the H-bonds follows the order S1—H2···N2 > N2—H2···S1 > N3—H3B···O1. The trend in this stability pattern is also found by comparing the ΔG_{298} values of the interactions.

Acknowledgments I would like to thank the reviewers for their helpful comments and suggestions to improve the manuscript.

References

1. Benson FR (1967) Tetrazoles, tetrazines and purines and related ring systems. In: Elderfield RC (ed) Heterocyclic compounds, vol 8. Wiley, New York, pp 1–104
2. Temple C Jr (1981) Triazoles 1, 2, 4. In: Montgomery JA (ed) Chemistry of the heterocyclic compounds, vol 37. Wiley, New York, pp 155–162
3. Unangst PC, Shrum GP, Connor DT, Dyer RD, Schrier DJ (1992) J Med Chem 35:3691–3698
4. Mullican MD, Wilson MW, Conner DT, Kostlan CR, Schrier DJ, Dyer RD (1993) J Med Chem 36:1090–1099
5. Jones DH, Slack R, Squires S, Wooldridge KRH (1965) J Med Chem 8:676–680
6. Sughen JK, Yoloye T (1978) Pharm Acta Helv 58:64–68
7. Shams El-Dine SA, Hazzaa AAB (1974) Pharmazie 29:761–763
8. Stillings MR, Welbourn AP, Walter DS (1986) J Med Chem 29:2280–2284
9. Sztanke K, Tuzimski T, Rzymowska J, Pasternak K, Kandefer-Szerszeń M (2008) Eur J Med Chem 43:404–419
10. Ilango K, Valentina P (2010) Pharm Chem 2:16–22
11. Demirbaş N, Ugurluoglu D, Demirbaş A (2002) Bioorg Med Chem 10:3717–3723
12. Kane JM, Dudley MW, Sorensen SM, Miller FP (1988) J Med Chem 31:1253–1258
13. Porsolt RD, Bertin A, Jalfre M (1977) Arch Int Pharmacodyn Ther 229:327–336
14. Vamvakides A (1990) Ann Pharm Fr 48:154–159
15. Vreugdenhil W, Haasnoot JG, Reedijk J, Spek AL (1987) Inorg Chim Acta 129:205–216
16. van Albada GA, de Graaff RAG, Haasnoot JG, Reedijk J (1984) Inorg Chem 23:1404–1408
17. Vos G, le Febre RA, de Graaff RAG, Haasnoot JG, Reedijk J (1983) J Am Chem Soc 105:1682–1683
18. Kahn O, Martinez CJ (1998) Science 279:44–48
19. Jeffrey GA (1997) An introduction to hydrogen bonding. Oxford University Press, New York
20. Scheiner S (1997) Hydrogen bonding. Oxford University Press, New York
21. Desiraju GR, Steiner T (1999) The weak hydrogen bond in structural chemistry and biology. Oxford University Press, Oxford
22. Zundel G (2000) Adv Chem Phys 111:1–217
23. Desiraju RG (1991) Acc Chem Res 24:290–296
24. Robertson EG, Simons JP (2001) Phys Chem Chem Phys 3:1–18
25. Wang YQ, Wang HG, Zhang SQ, Pei KM, Zheng X, Phillips DL (2006) J Chem Phys 125:214506–214512
26. Ahn DS, Lee S, Kim B (2004) Chem Phys Lett 390:384–388
27. Hunter KC, Rutledge LR, Wetmore SD (2005) J Phys Chem A 109:9554–9562
28. Douhal A, Kim SK, Zewail AH (1995) Nature 378:260–263
29. Sobolewski AL, Domcke W (2003) Chem Phys 294:73–83
30. Schultz T, Samoylova E, Radloff W, Hertel IV, Sobolewski AL, Domcke W (2004) Science 306:1765–1768
31. Bach A, Tanner C, Manca C, Frey HM, Leutwyler S (2003) J Chem Phys 119:5933–5942
32. Meuwly M, Bach A, Leutwyler S (2001) J Am Chem Soc 123:11446–11453
33. Casadesús R, Moreno M, Lluch JM (2003) Chem Phys 290:319–336
34. Lima MCP, Coutinho K, Canuto S, Rocha WR (2006) J Phys Chem A 110:7253–7261
35. Kurse LI, Finkelestein JA (1990) Eur Pat App Ep-395, 505 (Cl. C07 D401/60) Chem Abst (1990)113, 115311w
36. Elquero J, Marzin C, Katritzky AR, Linda P (1976) The tautomerism of heterocycles. Acedemic, New York, p 407
37. Shtefan ED, Vvedenskii VY (1996) Russ Chem Rev 65:307–314
38. Siwek A, Wujec M, Wawrzycka-Gorczyca I, Dobosz M, Paneth P (2008) Heteroat Chem 19(4):337–344
39. Potts KT (1961) Chem Rev 61(2):87–127
40. Chai B, Qian X, Cao S, Liu H, Song G (2003) Arkivoc ii:141–145
41. Zamani K, Faghihi K, Tofighi T, Shariatzadeh MR (2004) Turk J Chem 28(1):95–100
42. Davari MD, Bahrami H, Haghighi ZZ, Zahedi M (2010) J Mol Model 16:841–855
43. Peng C, Ayala PY, Schlegel HB, Frisch MJ (1996) J Comput Chem 17:49–56
44. Dennington R II, Keith T, Millam J (2007) GaussView, Version 4.1.2. Semichem Inc, Shawnee Mission
45. Frisch MJ, Trucks GW, Schlegel HB, Scuseria GE, Robb MA, Cheeseman JR, Montgomery JA Jr, Vreven T, Kudin KN, Burant JC, Millam JM, Iyengar SS, Tomasi J, Barone V, Mennucci B, Cossi M, Scalmani G, Rega N, Petersson GA, Nakatsuji H, Hada M, Ehara M, Toyota K, Fukuda R, Hasegawa J, Ishida M, Nakajima T, Honda Y, Kitao O, Nakai H, Klene M, Li X, Knox JE, Hratchian HP, Cross JB, Bakken V, Adamo C, Jaramillo J, Gomperts R, Stratmann RE, Yazyev O, Austin AJ, Cammi R, Pomelli C, Ochterski JW, Ayala PY, Morokuma K, Voth GA, Salvador P, Dannenberg JJ, Zakrzewski VG, Dapprich S, Daniels AD, Strain MC, Farkas O, Malick DK, Rabuck AD, Raghavachari K, Foresman JB, Ortiz JV, Cui Q, Baboul AG, Clifford S, Cioslowski J, Stefanov BB, Liu G, Liashenko A, Piskorz P, Komaromi I, Martin RL, Fox DJ, Keith T, Al-Laham MA, Peng CY, Nanayakkara A, Challacombe M, Gill PMW, Johnson B, Chen W, Wong MW, Gonzalez C, Pople JA (2004) Gaussian 03, Revision E.01. Gaussian Inc, Wallingford
46. Becke AD (1993) J Chem Phys 98:5648–5652
47. Lee C, Yang W, Parr RG (1988) Phys Rev B 37:785–789
48. Krishnan R, Binkley JS, Seeger R, Pople JA (1980) J Chem Phys 72:650–654
49. Frisch MJ, Pople JA, Binkley JS (1984) J Chem Phys 80:3265–3269
50. Latajka Z, Bouteiller Y (1994) J Chem Phys 101:9793–9799
51. Lundell J, Latajka Z (1997) J Phys Chem A 101:5004–5009
52. Dkhissi A, Adamowicz L, Maes G (2000) Chem Phys Lett 324:127–136

53. Chalasinski G, Szczesniak MM (1994) Chem Rev 94:1723–1765
54. Hobza P, Zahradnik R (1988) Chem Rev 88:871–897
55. van Duijneveldt FB, van Duijneveldt-van de Rijdt JGCM, van Lenthe JH (1994) Chem Rev 94:1873–1885
56. Boys SF, Bernardi F (1970) Mol Phys 19:553–566
57. Miertuš S, Scrocco E, Tomasi J (1981) Chem Phys 55:117–129
58. Barone V, Cossi M (1998) J Phys Chem A 102:1995–2001
59. Cossi M, Rega N, Scalmani G, Barone V (2003) J Comput Chem 24:669–681
60. Tomasi J, Mennucci B, Cammi R (2005) Chem Rev 105:2999–3093
61. Wei D, Salahub DR (1994) Chem Phys Lett 224:291–296
62. Surján P, Ángyán JG (1994) Chem Phys Lett 225:258–264
63. Moor WJ (1974) In: Physical Chemistry. Longman, pp 282–299
64. Atkins PW (1994) In: Physical Chemistry. Oxford University Press, pp 147–170
65. Dinçer M, Özdemir N, Çetin A, Cansız A, Şekerci M (2005) Acta Crystallogr E61:o3214–o3216
66. Bernstein J, Davis RE, Shimoni L, Chang NL (1995) Angew Chem Int Ed Engl 34:1555–1573
67. Delaere D, Raspoet G, Nguyen MT (1999) J Phys Chem A 103:171–177
68. Enchev V, Markova N, Angelova S (2007) Chem Phys Res J 1:1
69. Bats JW (1976) Acta Crystallogr B 32:2866–2870
70. Solimannejad M, Gharabaghi M, Scheiner S (2011) J Chem Phys 134:24312–24317
71. Solimannejad M, Scheiner S (2011) Int J Quantum Chem 111:3196–3200
72. Solimannejad M, Scheiner S (2009) Mol Phys 107:713–719
73. Yang Y (2009) Int J Quantum Chem 109:266–274
74. Biswal HS, Wategaonkar S (2009) J Phys Chem A 113:12774–12782
75. Leffler JE (1953) Science 117:340–341
76. Hammond GS (1955) J Am Chem Soc 77:334–338